



1 **Evidence for increased expression of the Amundsen Sea Low over the South Atlantic**
2 **during the late Holocene**

3

4 Zoë Thomas^{1,2,3}, Richard T. Jones^{4†}, Chris Fogwill^{1,2,5}, Jackie Hatton⁴, Alan Williams^{2,3,6}, Alan
5 Hogg⁷, Scott Mooney¹, Philip Jones^{8,9}, David Lister⁸, Paul Mayewski¹⁰ and Chris Turney^{1,2,3}

6

7 1. Palaeontology, Geobiology and Earth Archives Research Centre, School of Biological, Earth
8 and Environmental Sciences, University of New South Wales, Australia

9 2. Climate Change Research Centre, School of Biological, Earth and Environmental Sciences,
10 University of New South Wales, Australia

11 3. ARC Centre of Excellence in Australian Biodiversity and Heritage (CABAH), School of
12 Biological, Earth and Environmental Sciences, University of New South Wales, Sydney, Australia

13 4. Department of Geography, Exeter University, Devon, EX4 4RJ, United Kingdom

14 5. School of Geography, Geology and the Environment, Keele University, Staffordshire,
15 ST5 5BG, UK

16 6. College of Humanities, Arts & Social Sciences, Flinders University, Bedford Park, SA 5042,
17 Australia

18 7. Waikato Radiocarbon Laboratory, University of Waikato, Private Bag 3105, Hamilton, New
19 Zealand

20 8. Climatic Research Unit, School of Environmental Sciences, University of East Anglia, Norwich,
21 UK

22 9. Center of Excellence for Climate Change Research, Department of Meteorology, King
23 Abdulaziz University, Jeddah, 21589, Saudi Arabia

24 10. Climate Change Institute, University of Maine, Orono, ME, USA

25 †. Deceased.

26 * E-mail: z.thomas@unsw.edu.au

27



28 **Abstract:**

29 The Amundsen Sea Low (ASL) plays a major role in modulating the climate and environment of
30 Antarctica and is of global importance in the Earth system. Unfortunately, a relative dearth of
31 observational data across the Amundsen and Bellingshausen Seas prior to the satellite era
32 (post-1979) limits our understanding of past behaviour and impact of the ASL. The limited
33 proxy evidence for changes in the ASL are primarily limited to the Antarctic where ice core
34 evidence suggests a deepening of the atmospheric pressure system during the late Holocene.
35 However, no data has previously been reported from the northern side of the ASL. Here we
36 report a high-resolution, multi-proxy study of a 5000 year-long peat record from the Falkland
37 Islands (South Atlantic sector of the Southern Ocean), an area sensitive to contemporary ASL
38 dynamics. In combination with climate reanalysis, we find a marked period of wetter, colder
39 conditions most likely the result of enhanced southerly airflow between 5000 and 2500 years
40 ago, and inconsistent with synoptic conditions associated with the ASL today. After 2500 years
41 ago, drier and warmer conditions were established, implying more westerly airflow and the
42 increased projection of the ASL onto the South Atlantic. Our results are in agreement with
43 Antarctic ice core records and suggest the Falkland Islands provide a valuable location for
44 reconstructing atmospheric circulation changes across a large sector of the Southern Ocean on
45 multi-decadal to millennial timescales. The possible role of tropical Pacific in establishing
46 contemporary-like synoptic circulation is explored.

47



48 **1. Introduction**

49 The leading mode of variability in atmospheric circulation across the southern mid-high
50 latitudes is the Southern Annular Mode (SAM), manifested as the pressure difference between
51 65°S and 40°S (Marshall, 2003; Thompson et al., 2011). The multi-decadal trend to a more
52 positive SAM since the mid-20th century (Fogt et al., 2012; Hosking et al., 2013) is expressed by
53 a strengthening and poleward shift of mid-latitude westerly airflow and storm tracks over the
54 Southern Ocean (Marshall, 2003; Thompson et al., 2011; Visbeck, 2009), and has been linked to
55 changes in climate, ocean ventilation, air-sea carbon flux, sea ice trends, and ice sheet dynamics
56 on interannual to multi-decadal timescales (Jones et al., 2016a; Landschützer et al., 2015;
57 Pritchard et al., 2012; Le Quéré et al., 2007; Thomas et al., 2018). Whilst the SAM may dominate
58 contemporary climate across the mid latitudes, other climate modes and atmospheric patterns
59 also play important roles both spatially and temporally. Arguably the most important in this
60 regard is the Amundsen Sea Low (ASL), a quasi-stationary low-pressure system located in the
61 Amundsen and Bellingshausen Seas (45-75°S, 180-60°W) - a consequence of the Antarctic
62 Peninsula and regional topography that dynamically influences atmospheric flow across this
63 sector of the Southern Ocean (Fogt et al., 2012; Hosking et al., 2013; Turner et al., 2013). Proxy
64 reconstructions of SAM and/or associated westerly winds have been generated for the Holocene
65 (Abram et al., 2014; Dixon et al., 2012; Fletcher and Moreno, 2011; Mayewski et al., 2017;
66 Moreno et al., 2012; Sime et al., 2010; Turney et al., 2016c) but there is a relative dearth of
67 records for the past behaviour of the ASL (Mayewski et al., 2013).

68

69 Seasonally, the ASL migrates across the Bellingshausen Sea into the Ross Sea: during the austral
70 summer, the pressure minimum extends east to the Antarctic Peninsula (reaching its lowest
71 geopotential height off coastal West Antarctica in the Amundsen Sea), while in winter, the ASL
72 migrates to the west into the eastern Ross Sea (Fogt et al., 2012). As a result, the ASL plays a
73 dominant role in climate and environmental variability across the wider south Pacific sector of
74 the Southern Ocean (Kreutz et al., 2000; Turner et al., 2016), modulated by changes in the



75 tropical Pacific (Abram et al., 2014; Ding et al., 2011; Lachlan-cope and Connolley, 2006; Turney
76 et al., 2017). In particular, both the geopotential height and location of the ASL affects regional
77 synoptic conditions that extend into the interior of West Antarctica, (Clem et al., 2017; Ding et
78 al., 2011; Schneider et al., 2012). Across the period 1979-2008 (satellite era) the ASL appears to
79 have deepened, with suggested links to reduced sea ice along the western Antarctic Peninsula
80 and more broadly with climate changes across the southern Atlantic and Antarctic Peninsula
81 (Fogt et al., 2012; Raphael et al., 2016; Turner et al., 2013; Turney et al., 2016b).

82

83 The lack of long-term surface-based (*in situ*) observations in the Amundsen, Bellingshausen, and
84 Ross Seas severely limits our understanding of the properties and impact of the ASL on multi-
85 decadal to millennial timescales; an important consideration given uncertainties over the
86 response of the ASL to future anthropogenic forcing (IPCC, 2013). Fortunately, palaeoclimate
87 proxy data from the region integrated with reanalysis data offers an opportunity to identify
88 processes and mechanisms on timescales beyond those of satellite-era observations (since
89 1979). A major challenge for reconstructing changes in the ASL, however, is disentangling the
90 role of mid-latitude westerly airflow associated with SAM. The location of the palaeo records
91 and the proxies used are crucial in this regard. For instance, recent work from Siple Dome in
92 West Antarctic recognised increased delivery of sea salt sodium ($ssNa^+$) interpreted as
93 representing a deepening of the ASL, with a particularly marked trend since 2900 years ago
94 (hereafter 2.9 ka) (Mayewski et al., 2013). Although Siple Dome provides an important southern
95 'observation' point, information is needed on the northern side of the ASL to provide a more
96 complete reconstruction of its location and/or depth during the Holocene, as well a more
97 thorough understanding tropical Pacific-high latitude teleconnections. Here we report a new
98 high-resolution record of airflow extending the record over the past 5 ka and demonstrate a
99 marked change in synoptic conditions around 2.5 ka, providing important new insights into the
100 long-term behaviour of the ASL and the role of the tropic Pacific.

101



102 *1.1 Study site*

103 The Falkland Islands lie at 52°S, 540 km east of the coast of South America and 1500 km west of
104 subantarctic South Georgia. The present climate of the Falkland Islands is highly influenced by
105 the surrounding cool South Atlantic waters resulting in a cool temperate, maritime climate, with
106 corresponding low seasonality. Weather station data from the east Falkland Islands (Mount
107 Pleasant Airport) reveal a mean annual temperature of 5.5°C, high mean monthly and annual
108 wind speeds of ca. 8.5 m s⁻¹ (with prevailing westerly winds), and relatively low annual
109 precipitation of ca. 600 mm, distributed uniformly throughout the year (Lister and Jones, 2014).

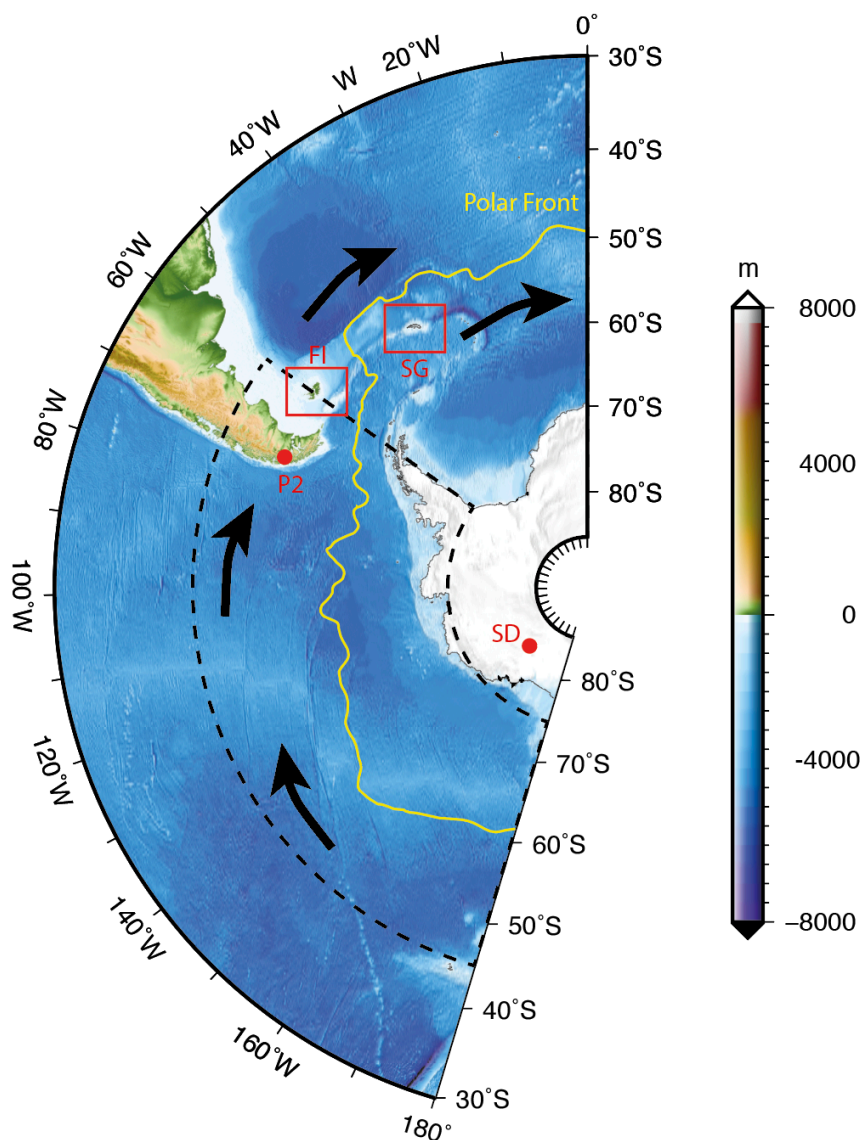
110

111 The Falkland Islands are dominated by extensive undulating lowlands, but several upland areas
112 in excess of 500 m above sea level (asl) occur within the archipelago. The islands are not
113 glaciated today and record only two periods of restricted glaciation in the Late Pleistocene
114 (Clapperton, 1971, 1990, 1993; Clapperton and Sugden, 1976; Roberts, 1984). Blanket peat was
115 established across large parts of the archipelago from 16.5 ka (Wilson et al., 2002). The islands
116 are situated within the main latitudinal belt of Southern Hemisphere westerly airflow (Barrow,
117 1978), and are therefore ideally placed to monitor changing Holocene wind strength across the
118 South Atlantic. The need to understand the climate impacts is an urgent one; recent studies have
119 suggested that with the projected increase in temperatures on the Falkland Islands, upland
120 species are highly vulnerable to climate change (Upson et al., 2016).

121

122 To investigate past airflow, a 1.5 m sequence was taken with a D-section corer from an exposed
123 Ericaceous-grass peatland on Canopus Hill (51.691°S, 57.785°W, approximately 30 m asl),
124 outside Port Stanley (35 km from Mount Pleasant Airport). The uniform dark-brown peat was
125 contiguously sampled for pollen, charcoal and comprehensive radiocarbon dating. Work at this
126 site has previously recognised the input of exotic pollen and charcoal derived from South
127 America (Turney et al., 2016), with changes to westerly airflow over the past ~2.5 ka.

128



129

130 **Figure 1.** Location of the Falkland Islands (FI), South Georgia [SG], Siple Dome [SD] and Palm2
131 [P2]. Dashed line denotes contemporary defined limits of the ASL domain (Fogt et al., 2012).
132 Location of the polar front (yellow line) and direction of the Southern Hemisphere westerly
133 winds (black arrows) are also shown. Map made using Generic Mapping Tools (GMT) (Wessel et
134 al., 2013).



135 **2. Methods**

136

137 *2.1 Pollen analysis*

138 The pollen samples were prepared using standard palynological techniques (Faegri and Iversen,
139 1975). Volumetric samples were taken every 1 cm along the core, with *Lycopodium* spores
140 added as a 'spike'. The samples were deflocculated with hot 10% NaOH and then sieved through
141 a 106 µm mesh, before acetolysis, to remove extraneous organic matter. The samples were
142 mounted in silicon oil and pollen types/palynomorphs were counted at 400× magnification
143 until a minimum of 300 target grains were identified. Pollen/palynomorphs were identified
144 using standard pollen keys (Barrow, 1978; Macphail and Cantrill, 2006) and the pollen type
145 slide collection at the University of Exeter, UK. The pollen counts were expressed as
146 percentages, with only total land pollen (TLP) contributing to the final pollen sum. The
147 *Lycopodium* 'spike' was also used to calculate total and individual pollen concentrations (grains
148 cm⁻³) (Stockmarr 1971), and these values were divided by the deposition time (year cm⁻¹) to
149 calculate pollen accumulation rates (PAR; grains cm⁻² year⁻¹). Major pollen zone boundaries
150 were determined using CONISS (stratigraphically constrained cluster analysis) (Grimm, 1987)
151 using the rioja package in R (Juggins, 2017).

152

153 *2.2 Charcoal analysis*

154 Past fire activity was investigated using counts of micro-charcoal fragments (< 106 µm)
155 identified on the pollen slides (Whitlock and Larsen, 2001). Counts were undertaken at each
156 level until a fixed total of 20 *Lycopodium* spores were counted and the total expressed as a
157 concentration (fragments per cm³). Charcoal accumulation rate (CHAR) was calculated by
158 dividing the total charcoal concentration by the deposition time estimated from the age-depth
159 relationship.

160

161



162 *2.3 Radiocarbon and ¹³⁷Cs dating*

163 To derive a chronological framework for the Canopus Hill peat sequence, terrestrial plant
164 macrofossils (fruits and leaves) were extracted. These macrofossils were given an acid–base–
165 acid (ABA) pre-treatment and then combusted and graphitised in the University of Waikato
166 AMS laboratory, with ¹⁴C/¹²C measurement by the University of California at Irvine (UCI) on a
167 NEC compact (1.5SDH) AMS system. The pre-treated samples were converted to CO₂ by
168 combustion in sealed pre-baked quartz tubes, containing Cu and Ag wire. The CO₂ was then
169 converted to graphite using H₂ and an Fe catalyst, and loaded into aluminium target holders for
170 measurement at UCI. The ¹⁴C measurements were supplemented by ¹³⁷Cs measurements near
171 the top of the profile to detect the onset of nuclear tests in the mid-20th century. ¹³⁷Cs analysis
172 was undertaken following standard techniques with measurements made using an ORTEC high-
173 resolution, low-background coaxial germanium detector. Detectable measurements were
174 obtained down to 8.5 and 9.5 cm and the lowest depth assigned an age of 1963, the time of early
175 radionuclide fallout at these latitudes (Hancock et al., 2011).

176

177 *2.4 Age modelling*

178 The ¹⁴C and ¹³⁷Cs ages were used to develop an age model using a P_{sequence} deposition model
179 in OxCal 4.2 (Bronk Ramsey, 2008; Bronk Ramsey and Lee, 2013); with the General Outlier
180 analysis detection method (probability=0.05) (Bronk Ramsey, 2009). The ¹⁴C ages were
181 calibrated against the Southern Hemisphere calibration (SHCal13) data set (Hogg et al., 2013).
182 The model was based on 1000 iterations, with the surface (depth zero) and year of sampling
183 (2010) as the uppermost chronological control point. The two basal ages were excluded due to
184 an age inversion, possibly a result of root penetration. Using Bayes' theorem, the algorithms
185 employed sample possible solutions with a probability that is the product of the prior and
186 likelihood probabilities (Bronk Ramsey, 2008). Taking into account the deposition model and
187 the actual age measurements, the posterior probability densities quantify the most likely age
188 distributions; the outlier option was used to detect ages that fall outside the calibration model



189 for each group, and if necessary, down-weight their contribution to the final age estimates.
 190 Modelled ages are reported here as thousands of calendar years before present (CE 1950) or ka
 191 (Table 1 and Figure 2). The multi-proxy sequence reported here spans the last 5 ka (Figure 2).
 192 We used the mean of the modelled age solutions to estimate the age of a fraction at each sample
 193 depth.
 194

Depth, cm	Wk lab number	Material	% Modern / ¹⁴ C BP ± 1 σ	Mean cal. years BP ± 1 σ
8-9	34598	Fruits and leaves	117.0±0.4%M	-21±15
9		¹³⁷ Cs		-19±14
11-12	32994	Fruits and leaves	107.8±0.4%M	-8±4
18-19	37007	Fruits and leaves	107.3±0.3%M	-3±12
25-26	35146	Fruits and leaves	95±25	86±63
35-36	37008	Fruits and leaves	647±25	603±29
39-40	33445	Fruits and leaves	761±25	661±27
57-58	32996	Fruits and leaves	1818±25	1682±50
70-71	32350	Fruits and leaves	2235±25	2215±58
97-98	32997	Fruits and leaves	2749±25	2810±33
107-108	32998	Fruits and leaves	2914±26	2997±57
120-121	41767	Fruits and leaves	3238±20	3416±31
141-142	32351	Fruits and leaves	3955±32	4352±66
148-149	41768	Fruits and leaves	4390±20	4908±42
153.5-154.5	42144	Fruits and leaves	4039±21	
156.5-157.5	42145	Fruits and leaves	4075±22	

195
 196 **Table 1.** Radiocarbon and modelled calibrated age ranges for the Canopus Hill peat sequences
 197 using the P_sequence and Outlier analysis option in OxCal 4.2 (Bronk Ramsey, 2008; Bronk
 198 Ramsey and Lee, 2013). The SHCal13 (Hogg et al., 2013) and Bomb04SH (Hua and Barbetti,
 199 2004) calibration curves were used. Note: calibrated ages are relative to Before Present (BP) i.e.
 200 CE 1950.

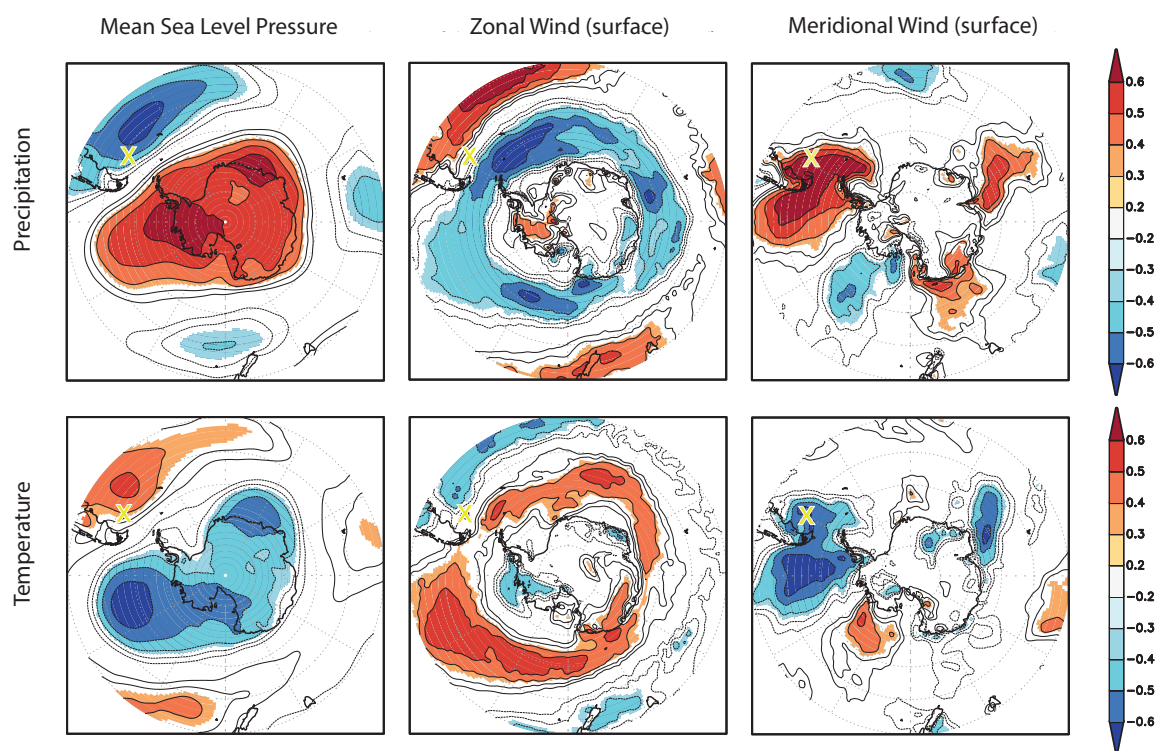


201 **3. Results and Discussion**

202

203 *3.1 Contemporary Climate*

204 Regional climate dynamics were explored using the ERA Interim reanalysis (Dee et al., 2011),
205 and the instrumental observations from Mount Pleasant Airport weather station on the
206 Falkland Islands (Jones et al., 2016b; Lister and Jones, 2014). Given the seasonal nature of
207 vegetation growth (including peat accumulation), spatial correlations using deseasonalised and
208 detrended spring-summer precipitation and temperature were investigated. These analyses
209 show important links with atmospheric synoptic conditions (Figure 2) including a clear link
210 between precipitation and zonal and meridional circulation (Figure 2c). Crucially, wetter
211 conditions are associated with a weakening of the ASL and the delivery of more southerly and
212 easterly airflow across the South Atlantic (Jones et al., 2016b). Conversely, more northerly
213 airflow is associated with less precipitation over the Falklands. A similar picture emerges with
214 variations in temperature (Figure 2a and d) with a deeper (i.e. more intense low pressure) ASL
215 associated with warmer temperatures over the Falkland Islands, and a weaker ASL with cooler
216 conditions.



217

218 **Figure 2.** Spatial correlation of relationships between precipitation, temperature and synoptic
219 conditions from Mount Pleasant Airport (October to March), Falkland Islands ('X'). Mean Sea
220 Level Pressure (MSLP), surface zonal wind and surface meridional wind correlated with
221 October to March precipitation (upper row) and temperature (lower row) using ERA-79 Interim
222 reanalysis (Dee et al., 2011) (1979–2013). Significance $p_{field} < 0.05$. Analyses were made with
223 KNMI Climate Explorer (van Oldenborgh and Burgers, 2005).

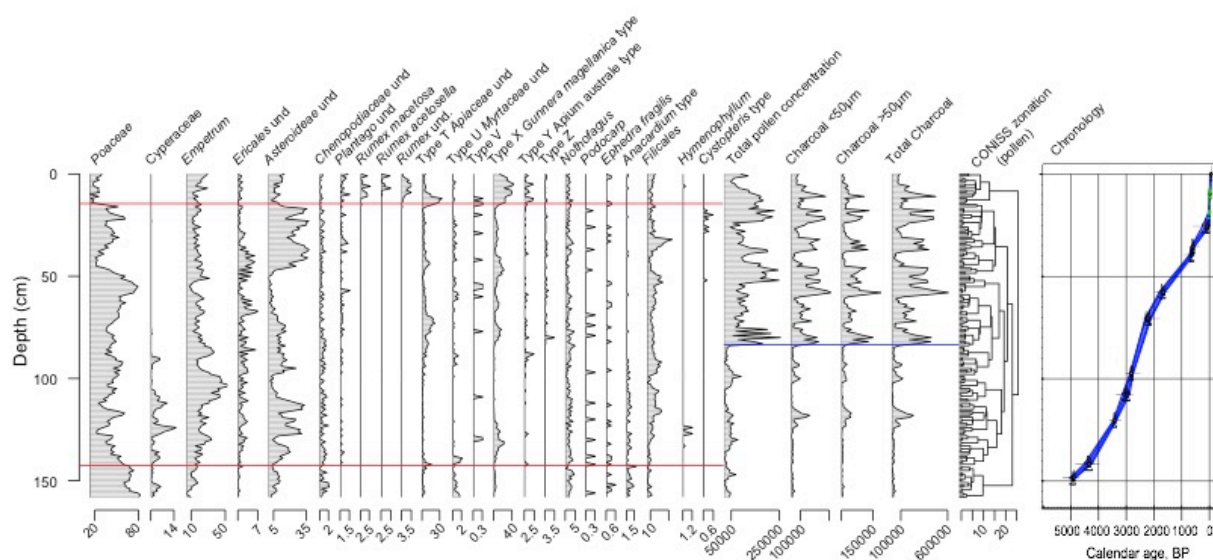


224 *3.2 Holocene Climate and Environmental Change*

225 The Canopus Hill peat sequence reported here from the Falkland Islands represents one of the
226 longest pollen records from the South Atlantic (Barrow, 1978; Turney et al., 2016a). Our
227 reconstruction appears to represent changing environmental conditions through the Holocene.
228 The pollen record through the mid- to late-Holocene is dominated by Poaceae and *Empetrum*,
229 consistent with both previous studies and current vegetation on the islands (Barrow, 1978;
230 Broughton and Mcadam, 2003; Clark et al., 1998; Turney et al., 2016a). However, in contrast to
231 these previous studies, we observe a major shift in the representation of Cyperaceae and the
232 total accumulation of pollen centred on ~2.5 ka (Figure 3).

233

234 Similar changes to the above are also observed in the aeolian transportation of exotic pollen and
235 charcoal derived from long-distance transport. These 'exotic' pollen in the Canopus Hill
236 sequence represent South American flora delivered to the site by westerly airflow. While only
237 representing between 0.3% and 4.6% of the pollen sum, we recorded *Nothofagus*, *Podocarpus*,
238 *Ephedra fragilis*, and *Anacardium*-type (arboreal) pollen grains. *Nothofagus* was the most
239 frequently recorded exotic taxon in the samples, due to its high representation on Tierra del
240 Fuego and the Islas de los Estados (upstream of the Falkland Islands), and high production of
241 wind-dispersed pollen that can be carried over long distances (Moreno et al., 2009). In extreme
242 situations, *Nothofagus* pollen has been recovered as far from South America as Marion Island
243 and Tristan da Cunha (Hafsten, 1960; Mildenhall, 1976; Wace and Dickson, 1965).



244

245 **Figure 3:** Summary pollen diagram from Canopus Hill, Port Stanley, with the left hand panels
 246 describing palynomorphs as percentages of the total land pollen plotted against depth. The
 247 middle panels show total pollen, charcoal of different size fractions and total charcoal expressed
 248 as a concentration (number cm^{-3}). The far right panel depicts the age-depth relationship, with
 249 1σ age range (blue envelope) and probability distributions generated from the Bayesian age
 250 model. Parallel lines denote major pollen (red) and charcoal/pollen concentration (blue) zone
 251 boundaries were determined using CONISS (Grimm, 1987).



252 Differences in the exotic pollen assemblages can reflect either changes in the transport pathway
253 (i.e. direction and wind strength) or regional vegetation change in the source area(s). Today,
254 *Nothofagus* dominates lowland Patagonian vegetation and is found throughout Patagonian Late
255 Glacial sequences. This taxa is thought to have been most widely established by 5 ka (Iglesias et
256 al., 2014; Kilian and Lamy, 2012), with a reasonably constant representation until stepped
257 expansion at Lago Guanaco, almost directly west of the Falklands (51.03°S, 72.83°W, 185m asl),
258 centred on 570 cal. years (Moreno et al., 2009; Villa-martínez et al., 2012). Fire activity and the
259 introduction of exotic weeds introduced by European settlers is thought to have resulted in the
260 rapid decline of *Nothofagus* at the end of the 19th century (Moreno et al., 2009).

261

262 Highly variable charcoal counts were obtained through the sequence, however, more than 99%
263 of charcoal fragments were less than 50 µm in size, with negligible amounts identified in the 50–
264 106 µm and >106 µm fractions (Figure 3). As charcoal of this size can be transported long
265 distances (Clark, 1988) it is likely that this influx of charcoal predominantly represent South
266 American sources and westerly (and south-westerly) airflow, and that there was little or no fire
267 in the local environment throughout the mid- to late-Holocene, The aeolian delivery of the
268 charcoal to the Falkland Islands is supported by the close correspondence between the Canopus
269 Hill and Lago Guanaco, Southwest Patagonia (Moreno et al., 2009) charcoal records. There is a
270 weak correlation between charcoal and *Nothofagus*, particularly in the younger half of the
271 record probably reflecting the similar transport modes. Recent syntheses of charcoal
272 stratigraphies across Patagonia have detected regional trends in biomass burning during the
273 Holocene with a moderate increase occurring over the last 3000 years (Huber et al., 2004;
274 Whitlock et al., 2007; Power et al., 2008).

275

276 3.3 Holocene changes in the Amundsen Sea Low (ASL)

277 Our results support the notion of pervasive westerly winds throughout the mid- to late-
278 Holocene, as shown by the consistent representation of *Nothofagus* pollen, as well as the pollen



279 of other rare exotic taxa including *Podocarp*, *Ephedra fragilis* and *Anacardium*-type found
280 throughout the Canopus Hill peat sequence. Whilst the presence of *Nothofagus* implies westerly
281 airflow has been maintained across the South Atlantic, the relatively high expression of
282 Cyperaceae between 5 and ~2.5 ka (Figure 4) suggests enhanced delivery of cooler and moister
283 air to the Falklands. Our analyses imply these conditions could have been brought about by
284 more southerly airflow across the South Atlantic (Figure 2), synoptic conditions inconsistent
285 with today's expression of the ASL. The marked decline in Cyperaceae and increase in charcoal
286 at ~2.5 ka indicates a shift to drier and potentially warmer conditions, most probably a result of
287 reduced southerly airflow and the northward movement and/or expansion of the ASL. The
288 inferred increase in primary productivity and pollen accumulation on the islands supports this
289 interpretation (Turney et al., 2016b).

290

291 These results compliment other studies from the broader South Atlantic region (Figure 4). Ice
292 core-derived proxies from Siple Dome, located in a key region for understanding ASL dynamics,
293 imply distinct changes in atmospheric circulation. Here, $ssNa^+$ provides a measure of sea-salt
294 species, the transport of which is significantly influenced by the ASL (Kreutz et al., 2000), with
295 higher values associated with a deeper ASL. The increase of $ssNa^+$ over the mid- to late Holocene
296 (~2.9 ka) thus implies a deepening of the ASL (Mayewski et al., 2013) consistent with our data.
297 The slight difference in the timing between these records may be a consequence of
298 chronological uncertainties or a lag in the projection of the ASL onto the South Atlantic (possibly
299 reflecting an eastward migration/extension of the ASL to where it is more commonly located
300 today). Farther north, the marine sequence from the PALM2 within the Skyring fjord system
301 east of the Andean crest of South America shows strong fluctuations of biogenic carbonate
302 accumulation rates in superficial fjord waters (Lamy et al., 2010). Carbonate preservation in
303 this record is interpreted to be a proxy for salinity changes as a result of prevailing westerly
304 winds that keep the low-salinity waters inside the fjord; lower salinity anomalies therefore
305 suggest stronger westerly winds. Intriguingly, the PALM2 record shows a pronounced sustained

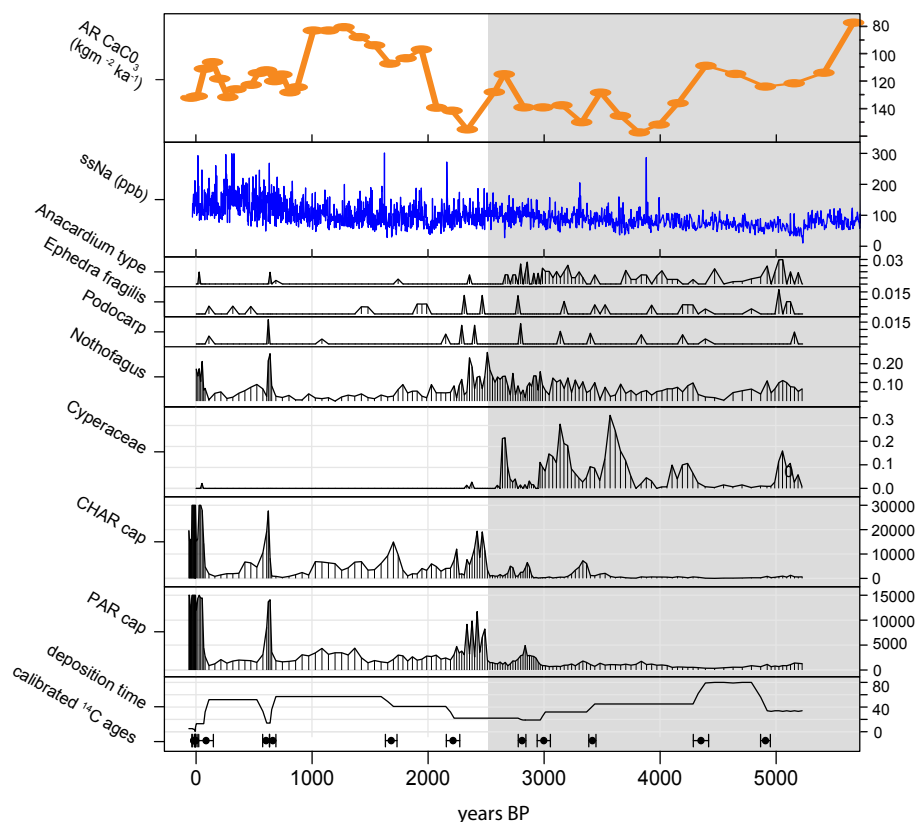


306 decrease in salinity anomalies from ~2.5 ka, interpreted to be a result of a strengthening of mid-
307 latitude westerly winds, consistent with our reconstruction.

308

309 Taken together the above results imply that there was a long-term change in the behaviour of
310 the ASL with the establishment of contemporary synoptic conditions around 2.5 ka. The reason
311 for a change at ~2.5 ka is not immediately apparent but one possibility is the tropical Pacific.
312 Today, equatorial Pacific ocean-atmospheric linkages are known to modulate the ASL with
313 associated impacts across the broader region including climate, sea ice and ice sheet dynamics
314 (Abram et al., 2014; Ding et al., 2011; Lachlan-cope and Connolley, 2006; Turney et al., 2017).
315 Reconstructions of sea surface temperatures and precipitation suggest the establishment of
316 more pervasive El Niño-Southern Oscillation (ENSO) activity from 3 to 2.5 ka (Carre et al., 2014;
317 Moy et al., 2002), that may have been projected onto the southeast Pacific sector of the Southern
318 Ocean (Abram et al., 2014). Given the projected increase in extreme ENSO events under future
319 anthropogenic forcing (Cai et al., 2015) further work is needed to determine the mechanisms,
320 timing and impacts of these low to high latitude teleconnections through the Holocene (Thomas,
321 2016).

322



323

324 **Figure 4:** Key data from the Canopus Hill sequence (Falkland Islands) and other South Atlantic
 325 records. From bottom to top: deposition time, total pollen accumulation rate (PAR), total
 326 charcoal accumulation rate (CHAR), *Cyperaceae*, *Nothofagus*, *Podocarp*, *Ephedra*, *Anacardium*-
 327 type re-expressed as accumulation rates, ssNa⁺ from Siple Dome (Mayewski et al., 2013) and
 328 salinity anomalies from PALM2 (Lamy et al., 2010). Calibrated radiocarbon ages and 1σ range
 329 are plotted at the base of the figure. Note that PAR and CHAR have both been capped at the
 330 modern end due to high accumulation rate. The grey boxed area marks the period during which
 331 there was limited expression of the ASL over the South Atlantic.

332

333



334 **4. Conclusion**

335

336 Whilst the Southern Annular Mode (SAM) dominates climate variability in the mid-latitudes of
337 the Southern Hemisphere, other climate modes and atmospheric patterns play important roles,
338 some of which are of global significance. One of the most important is the atmospheric pressure
339 centre known as the Amundsen Sea Low (ASL). Unfortunately, there are limited observational
340 and proxy datasets capturing the long-term behaviour and impact of the ASL. Here we report a
341 comprehensively dated peat record from Canopus Hill (Falkland Islands) in the South Atlantic
342 Ocean, a region highly sensitive to the ASL. Our multi-proxy study including pollen (including
343 wind-blown exotic taxa originating from South America) and charcoal allows us to reconstruct
344 climate changes over the last 5000 years. We observe a marked shift from pervasive wet and
345 cool to drier and warmer conditions around 2500 years ago. ERA Interim reanalysis suggests
346 this change was a consequence of the establishment of contemporary westerly airflow
347 associated with the ASL projecting onto the South Atlantic. The timing of this change is
348 consistent with increased surface warming and expression of the El Niño-Southern Oscillation
349 (ENSO) in the region, suggesting a strengthening of equatorial-high latitude atmospheric
350 teleconnections. Our study demonstrates the value of the Falkland Islands for reconstructing
351 atmospheric circulation changes across a large sector of the Southern Ocean on multi-decadal to
352 millennial timescales.

353

354

355 **Acknowledgements**

356 We would like to acknowledge the incredible debt we owe to our close friend and colleague
357 Richard Jones without whom this work would not have been possible. We will miss you Richard.
358 This project was supported by the Australian Research Council (FL100100195 and
359 DP130104156). We thank the Falkland Islands Government for permission to undertake



360 sampling on the island (permit number R07/2011) and Darren Christie for assisting with the
361 fieldwork.

362

363

364 **References**

365 Abram, N. J., Mulvaney, R., Vimeux, F., Phipps, S. J., Turner, J. and England, M. H.: Evolution of the
366 Southern Annular Mode during the past millennium, *Nat. Clim. Chang.*, 4(7), 1–6,
367 doi:10.1038/NCLIMATE2235, 2014.

368 Barrow, C.: Postglacial pollen diagrams from south Georgia (sub-Antarctic) and West Falkland
369 island (South Atlantic), *J. Biogeogr.*, 5(3), 251–274, doi:10.2307/3038040, 1978.

370 Bronk Ramsey, C.: Deposition models for chronological records, *Quat. Sci. Rev.*, 27(1–2), 42–60,
371 doi:10.1016/j.quascirev.2007.01.019, 2008.

372 Bronk Ramsey, C.: Dealing with outliers and offsets in radiocarbon dating, *Radiocarbon*, 51(3),
373 1023–1045, 2009.

374 Bronk Ramsey, C. and Lee, S.: Recent and Planned Developments of the Program OxCal,
375 *Radiocarbon*, 55(2–3), 720–730, doi:10.2458/azu_js_rc.55.16215, 2013.

376 Broughton, D. A. and Mcadam, J. H.: The current status and distribution of the Falkland Islands
377 pteridophyte flora, *Fern Gaz.*, 17(1), 21–38, 2003.

378 Cai, W., Santoso, A., Wang, G., Yeh, S., An, S., Cobb, K. M., Collins, M., Guilyardi, E., Jin, F., Kug, J.,
379 Lengaigne, M. and Mcphaden, M. J.: ENSO and greenhouse warming, *Nat. Clim. Chang.*, 5(9), 849–
380 859, doi:10.1038/nclimate2743, 2015.

381 Carre, M., Sachs, J. P., Purca, S., Schauer, A. J., Braconnot, P., Angeles Falcon, R., Julien, M. and
382 Lavallee, D.: Holocene history of ENSO variance and asymmetry in the eastern tropical Pacific,
383 *Science* (80-.), 345(6200), 1045–1048, 2014.

384 Clark, J. S.: Particle Motion and the Theory of Charcoal Analysis: Source Area, Transport,
385 Deposition, and Sampling, *Quat. Res.*, 30, 67–80, 1988.

386 Clark, R., Huber, U. M. and Wilson, P.: Late Pleistocene sediments and environmental change at



- 387 Plaza Creek, Falkland Islands, South Atlantic, *J. Quat. Sci.*, 13(2), 95–105,
388 doi:10.1002/(SICI)1099-1417(199803/04)13:2<95::AID-JQS351>3.0.CO;2-G, 1998.
- 389 Dee, D. P., Uppala, S. M., Simmons, A. J., Berrisford, P., Poli, P., Kobayashi, S., Andrae, U.,
390 Balmaseda, M. A., Balsamo, G., Bauer, P., Bechtold, P., Beljaars, A. C. M., van de Berg, L., Bidlot, J.,
391 Bormann, N., Delsol, C., Dragani, R., Fuentes, M., Geer, A. J., Haimberger, L., Healy, S. B., Hersbach,
392 H., H??lm, E. V., Isaksen, L., K??llberg, P., K??hler, M., Matricardi, M., McNally, A. P., Monge-Sanz, B.
393 M., Morcrette, J. J., Park, B. K., Peubey, C., de Rosnay, P., Tavolato, C., Th??paut, J. N. and Vitart, F.:
394 The ERA-Interim reanalysis: Configuration and performance of the data assimilation system, *Q.*
395 *J. R. Meteorol. Soc.*, 137(656), 553–597, doi:10.1002/qj.828, 2011.
- 396 Ding, Q., Steig, E. J., Battisti, D. S. and Küttel, M.: Winter warming in West Antarctica caused by
397 central tropical Pacific warming, *Nat. Geosci.*, 4(6), 398–403, doi:10.1038/ngeo1129, 2011.
- 398 Dixon, D. A., Mayewski, P. A., Goodwin, I. D., Marshall, G. J., Freeman, R., Maasch, A. and Sneed, S.
399 B.: An ice-core proxy for northerly air mass incursions into West Antarctica, *Int. J. Climatol.*, 32,
400 1455–1465, doi:10.1002/joc.2371, 2012.
- 401 Faegri, K. and Iverson, J.: *Textbook of pollen analysis*, Blackwell, Oxford., 1975.
- 402 Fletcher, M.-S. and Moreno, P. I.: Have the Southern Westerlies changed in a zonally symmetric
403 manner over the last 14,000 years? A hemisphere-wide take on a controversial problem, *Quat.*
404 *Int.*, 253(2012), 32–46, doi:10.1016/j.quaint.2011.04.042, 2011.
- 405 Fogt, R. L., Wovrosh, A. J., Langen, R. A. and Simmonds, I.: The characteristic variability and
406 connection to the underlying synoptic activity of the Amundsen-Bellingshausen Seas Low, *J.*
407 *Geophys. Res. Atmos.*, 117(7), 1–22, doi:10.1029/2011JD017337, 2012.
- 408 Grimm, E. C.: CONISS: A Fortran 77 Program for stratigraphically constrained cluster analysis by
409 the method of incremental sum of squares, *Comput. Geosci.*, 13(1), 13–35, 1987.
- 410 Hafsten, U.: The Quaternary history of vegetation in the South Atlantic Islands, *Philos. Trans. R.*
411 *Soc. B*, 152(949), 516–529, doi:10.1098/rspb.1960.0059, 1960.
- 412 Hogg, A. G., Hua, Q., Blackwell, P. G., Niu, M., Buck, C. E., Guilderson, T. P., Heaton, T. J., Palmer, J.
413 G., Reimer, P. J., Reimer, R. W., Turney, C. S. M. and Zimmerman, S. R. H.: SHCAL13 Southern



- 414 Hemisphere calibration , 0–50,000 years cal BP, *Radiocarbon*, 55(4), 1889–1903, 2013.
- 415 Hosking, J. S., Orr, A., Marshall, G. J., Turner, J. and Phillips, T.: The influence of the amundsen-
416 bellingshausen seas low on the climate of West Antarctica and its representation in coupled
417 climate model simulations, *J. Clim.*, 26(17), 6633–6648, doi:10.1175/JCLI-D-12-00813.1, 2013.
- 418 Hua, Q. and Barbetti, M.: Review of tropospheric bomb 14C data for carbon cycle modeling and
419 age calibration purposes, *Radiocarbon*, 46(4), 1273–1298, 2004.
- 420 IPCC: Climate Change 2013: The Physical Science Basis. Contribution of Working Group I to the
421 Fifth Assessment Report of the Intergovernmental Panel on Climate Change [], edited by T. F.
422 Stocker, D. Qin, G.-K. Plattner, M. Tignor, S. K. Allen, J. Boschung, A. Nauels, Y. Xia, V. Bex, and P.
423 M. Midgley, Cambridge University Press, Cambridge, United Kingdom and New York NY, USA.,
424 2013.
- 425 Jones, J. M., Gille, S. T., Goosse, H., Abram, N. J., Canziani, P. O., Charman, D. J., Clem, K. R., Crosta,
426 X., Lavergne, C. de, Eisenman, I., England, M. H., Fogt, R. L., Frankcombe, L. M., Marshall, G. J.,
427 Masson-Delmotte, V., Morrison, A. K., Orsi, A. J., Raphael, M. N., Renwick, J. A., Schneider, D. P.,
428 Simpkins, G. R., Steig, E. J., Stenni, B., Swingedouw, D. and Vance, T. R.: Assessing recent trends in
429 high-latitude Southern Hemisphere surface climate, *Nat. Clim. Chang.*, 6(10), In press,
430 doi:10.1038/nclimate3103, 2016a.
- 431 Jones, P. D., Harpham, C. and Lister, D.: Long-term trends in gale days and storminess for the
432 Falkland Islands, *Int. J. Climatol.*, 36(3), 1413–1427, doi:10.1002/joc.4434, 2016b.
- 433 Juggins, S.: rioja: Analysis of Quaternary Science Data, R package, [online] Available from:
434 <http://cran.r-project.org/package=rioja>, 2017.
- 435 Kreutz, K. J., Mayewski, P. A., Pittalwala, I. , Meeker, L. D., Twickler, M. S. and Whitlow, S. I.: Sea
436 level pressure variability in the Amundsen Sea region inferred from a West Antarctic
437 glaciochemical record, *J. Geophys. Res.*, 105(D3), 4047–4059, 2000.
- 438 Lachlan-cope, T. and Connolley, W.: Teleconnections between the tropical Pacific and the
439 Amundsen- Bellinghausens Sea: Role of the El Nino / Southern Oscillation, *J. Geophys. Res.*, 111,
440 D23101, doi:10.1029/2005JD006386, 2006.



- 441 Lamy, F., Kilian, R., Arz, H. W., Francois, J., Kaiser, J. and Prange, M.: Holocene changes in the
442 position and intensity of the southern westerly wind belt, *Nat. Geosci.*, 3(10), 695–699,
443 doi:10.1038/ngeo959, 2010.
- 444 Landschützer, P., Gruber, N., Haumann, F. A., Rödenbeck, C., Bakker, D. C. E., Heuven, S. Van,
445 Hoppema, M., Metzl, N., Sweeney, C. and Takahashi, T.: The reinvigoration of the Southern Ocean
446 carbon sink, *Science* (80-.), 349(6253), 1221–1224, 2015.
- 447 Lister, D. H. and Jones, P. D.: Long-term temperature and precipitation records from the
448 Falkland Islands, *Int. J. Climatol.*, 35(7), 1224–1231, doi:10.1002/joc.4049, 2014.
- 449 Marshall, G. J.: Trends in the Southern Annular Mode from observations and reanalyses, *J. Clim.*,
450 16(24), 4134–4143, doi:10.1175/1520-0442(2003)016<4134:TITSAM>2.0.CO;2, 2003.
- 451 Mayewski, P. A., Carleton, A. M., Birkel, S. D., Dixon, D., Kurbatov, A. V., Korotkikh, E., McConnell, J.,
452 Curran, M., Cole-dai, J., Jiang, S. and Plummer, C.: Ice core and climate reanalysis analogs to
453 predict Antarctic and Southern Hemisphere climate changes, *Quat. Sci. Rev.*, 155, 50–66,
454 doi:10.1016/j.quascirev.2016.11.017, 2017.
- 455 Mayewski, P. A., Maasch, K. A., Dixon, D., Sneed, S. B., Oglesby, R., Korotkikh, E., Potocki, M.,
456 Grigholm, B., Kreutz, K., Kurbatov, A. V., Spaulding, N., Stager, J. C., Taylor, K. C., Steig, E. J., White,
457 J., Bertler, N. A. N. and Jan, R.: West Antarctica' s Sensitivity to Natural and Human-forced
458 Climate Change Over the Holocene, *J. Quat. Sci.*, 28(1), 40–48, doi:10.1002/jqs.2593, 2013.
- 459 Mildenhall, D. C.: Exotic pollen rain on the Chatham Islands during the late pleistocene, *New
460 Zeal. J. Geol. Geophys.*, 19(3), 327–333, doi:10.1080/00288306.1976.10423562, 1976.
- 461 Moreno, P. I., François, J. P., Villa-Martinez, R. P. and Moy, C. M.: Millennial-scale variability in
462 Southern Hemisphere westerly wind activity over the last 5000 years in SW Patagonia, *Quat. Sci.
463 Rev.*, 28, 25–38, doi:10.1016/j.quascirev.2008.10.009, 2009.
- 464 Moreno, P. I., Villa-martínez, R., Cárdenas, M. L. and Sagredo, E. A.: Deglacial changes of the
465 southern margin of the southern westerly winds revealed by terrestrial records from SW
466 Patagonia (52 S), *Quat. Sci. Rev.*, 41, 1–21, doi:10.1016/j.quascirev.2012.02.002, 2012.
- 467 Moy, C. M., Seltzer, G. O., Rodbell, D. T. and Anderson, D. M.: Variability of El Nino/Southern



- 468 Oscillation activity at millennial timescales during the Holocene epoch, *Nature*, 420(November),
469 doi:10.1038/nature01163.1., 2002.
- 470 van Oldenborgh, G. J. and Burgers, G.: Searching for decadal variations in ENSO precipitation
471 teleconnections, *Geophys. Res. Lett.*, 32(15), 1–5, doi:10.1029/2005GL023110, 2005.
- 472 Pritchard, H. D., Ligtenberg, S. R. M., Fricker, H. A., Vaughan, D. G., Broeke, M. R. Van Den and
473 Padman, L.: Antarctic ice-sheet loss driven by basal melting of ice shelves, *Nature*, 484(7395),
474 502–505, doi:10.1038/nature10968, 2012.
- 475 Le Quéré, C., Rödenbeck, C., Buitenhuis, E. T., Conway, T. J., Langenfelds, R., Gomez, A.,
476 Labuschagne, C., Ramonet, M., Nakazawa, T., Metzl, N., Gillett, N. and Heimann, M.: Saturation of
477 the Southern Ocean CO₂ Sink Due to Recent Climate Change, *Science* (80-.), 316(1994), 1735–
478 1738, 2007.
- 479 Raphael, M. N., Marshall, G. J., Turner, J., Fogt, R. L., Schneider, D., Dixon, D. A., Hosking, J. S.,
480 Jones, J. M. and Hobbs, W. R.: THE AMUNDSEN SEA LOW: Variability, Change, and Impact on
481 Antarctic Climate, *Bull. Am. Meteorol. Soc.*, January, 111–122, doi:10.1175/BAMS-D-14-00018.1,
482 2016.
- 483 Schneider, D. P., Deser, C. and Okumura, Y.: An assessment and interpretation of the observed
484 warming of West Antarctica in the austral spring, *Clim. Dyn.*, 38, 323–347, doi:10.1007/s00382-
485 010-0985-x, 2012.
- 486 Sime, L. C., Kohfeld, K. E., Le, C., Wolff, E. W., Boer, A. M. De, Graham, R. M. and Bopp, L.: Southern
487 Hemisphere westerly wind changes during the Last Glacial Maximum : model-data comparison,
488 *Quat. Sci. Rev.*, 64(2013), 104–120, doi:10.1016/j.quascirev.2012.12.008, 2010.
- 489 Thomas, Z. A.: Using natural archives to detect climate and environmental tipping points in the
490 Earth System, *Quat. Sci. Rev.*, 152, 60–71, doi:10.1016/j.quascirev.2016.09.026, 2016.
- 491 Thomas, Z., Turney, C., Allan, R., Colwell, S., Kelly, G., Lister, D., Jones, P., Beswick, M., Alexander,
492 L., Lippmann, T., Herold, N. and Jones, R.: A new daily observational record from Grytviken,
493 South Georgia: exploring 20th century extremes in the South Atlantic, *J. Clim.*, 31, 1743–1755,
494 doi:10.1175/JCLI-D-17-0353.1, 2018.



- 495 Thompson, D. W. J., Solomon, S., Kushner, P. J., England, M. H., Grise, K. M. and Karoly, D. J.:
496 Signatures of the Antarctic ozone hole in Southern Hemisphere surface climate change, *Nat.*
497 *Geosci.*, 4(11), 741–749, doi:10.1038/ngeo1296, 2011.
- 498 Turner, J., Lu, H., White, I., King, J. C., Phillips, T., Hosking, J. S., Bracegirdle, T. J., Marshall, G. J.,
499 Mulvaney, R. and Deb, P.: Absence of 21st century warming on Antarctic Peninsula consistent
500 with natural variability, *Nature*, 535(7612), 411–415, doi:10.1038/nature18645, 2016.
- 501 Turner, J., Phillips, T., Hosking, J. S., Marshall, G. J. and Orr, A.: The Amundsen Sea low, *Int. J.*
502 *Bifurc. Chaos*, 1829, 1818–1829, doi:10.1002/joc.3558, 2013.
- 503 Turney, C., Jones, R., Fogwill, C., Hatton, J., Williams, a. N., Hogg, A., Thomas, Z., Palmer, J. and
504 Mooney, S.: A 250 year periodicity in Southern Hemisphere westerly winds over the last 2600
505 years, *Clim. Past*, 12, 189–200, doi:10.5194/cpd-11-2159-2015, 2016a.
- 506 Turney, C. S. M., Fogwill, C. J., Palmer, J. G., Sebille, E. Van, Thomas, Z., Mcglone, M., Richardson, S.,
507 Wilmshurst, J. M., Fenwick, P., Zunz, V., Goosse, H., Wilson, K., Carter, L., Lipson, M., Jones, R. T.,
508 Harsch, M. and Clark, G.: Tropical forcing of increased Southern Ocean climate variability
509 revealed by a 140-year subantarctic temperature reconstruction, *Clim. Past*, 13, 231–248,
510 doi:10.5194/cp-13-231-2017, 2017.
- 511 Turney, C. S. M., Jones, R. T., Lister, D., Jones, P., Williams, A. N., Hogg, A., Thomas, Z. A., Compo,
512 G. P., Yin, X., Fogwill, C. J., Palmer, J., Colwell, S., Allan, R. and Visbeck, M.: Anomalous mid-
513 twentieth century atmospheric circulation change over the South Atlantic compared to the last
514 6000 years, *Environ. Res. Lett.*, 11(6), 64009, doi:10.1088/1748-9326/11/6/064009, 2016b.
- 515 Turney, C. S. M., Wilmshurst, J. M., Jones, R. T., Wood, J. R., Palmer, J. G., Hogg, A. G., Fenwick, P.,
516 Crowley, S. F., Privat, K. and Thomas, Z.: Reconstructing atmospheric circulation over southern
517 New Zealand: Establishment of modern westerly air flow 5500 years ago and implications for
518 Southern Hemisphere Holocene climate change, *Quat. Sci. Rev.*, 159(2017), 77–87,
519 doi:10.1016/j.quascirev.2016.12.017, 2016c.
- 520 Upson, R., Williams, J. J., Wilkinson, T. P., Clubbe, C. P., Ilya, M., Maclean, D., Mcadam, J. H. and
521 Moat, J. F.: Potential Impacts of Climate Change on Native Plant Distributions in the Falkland



- 522 Islands, PLoS One, 11, e0167026., doi:10.1371/journal.pone.0167026, 2016.
- 523 Villa-martínez, R., Moreno, P. I. and Valenzuela, M. A.: Deglacial and postglacial vegetation
524 changes on the eastern slopes of the central Patagonian Andes (47 S), Quat. Sci. Rev., 32(2012),
525 86–99, doi:10.1016/j.quascirev.2011.11.008, 2012.
- 526 Visbeck, M.: A station-based southern annular mode index from 1884 to 2005, J. Clim., 22(4),
527 940–950, doi:10.1175/2008JCLI2260.1, 2009.
- 528 Wace, N. . and Dickson, J. .: Part II. The terrestrial botany of the Tristan da Cunha Islands, Philos.
529 Trans. R. Soc. B, 249, 273–360, doi:10.1098/rstb.1965.0014, 1965.
- 530 Wessel, P., Smith, W. H. F., Scharroo, R., Luis, J. and Wobbe, F.: Generic Mapping Tools: Improved
531 Version Released, Eos, Trans. Am. Geophys. Union, 94(45), 409–410,
532 doi:10.1002/2013E0450001, 2013.
- 533 Wilson, P., Clark, R., Birnie, J. and Moore, D. M.: Late Pleistocene and Holocene landscape
534 evolution and environmental change in the Lake Sullivan area, Falkland Islands, South Atlantic,
535 Quat. Sci. Rev., 21(16–17), 1821–1840, doi:10.1016/S0277-3791(02)00008-2, 2002.
- 536